Studying Resolved Stellar Populations with the James Webb Space Telescope

T. Brown[1], H. Ferguson[1], J. Gardner[2], L.Greggio[3], H. B. Hammel[4], A. Renzini[3], M. Rich[5], H. Richer[6], M. Stiavelli[1,7] (editor), R. Wyse[7]

Version 4.4 – 10/22/2008

1 Space Telescope Science Institute, 3700 San Martin Dr., Baltimore, MD 21218, USA
2 Laboratory for Observational Cosmology, Code 665, Goddard Space Flight Center, Greenbelt, MD 20771, USA
3 INAF, Osservatorio Astronomico di Padova, Vicolo dell'Osservatorio 5, I35122, Padova, Italy
4 Space Science Institute, 4750 Walnut Avenue, Suite 205, Boulder, CO 80301, USA
5 Dept. of Physics and Astronomy, University of California, Los Angeles, CA 90095, USA
6 Dept. of Physics and Astronomy, University of British Columbia, Vancouver, BC, Canada
7 Dept. of Physics and Astronomy, Johns Hokins University, 3900 North Charles Street, Baltimore, MD 21218, USA

Abstract

The James Webb Space Telescope (JWST) will be an exciting, highly capable tool, able to make important contributions to studies of stellar populations in nearby galaxies, including our own. JWST observations will contribute to: (1) the study of the star formation histories of nearby galaxies, exploiting the large lever arm provided by visible-infrared colors; (2) the derivation of the properties of stellar populations from the study of the bright red stellar component out to the Virgo cluster and beyond; and (3) the derivation of the white dwarf cooling sequence age of globular clusters in the Milky Way from the study of deep visible red color magnitude diagrams.

1. Introduction

One of the core goals of the James Webb Space Telescope (JWST) is to determine the history of star formation and metal enrichment in the Universe. JWST will pursue this goal primarily by searching for luminous objects at very high redshift. An important complement to the high-redshift observations will be studies of stellar populations in nearby galaxies, including our own, to determine the star formation history of these objects, to characterize the evolution of heavy elements and to determine the age of the oldest stellar populations.

JWST was not designed to carry out studies of resolved stellar populations at visible wavelengths: its optical quality is fixed by the requirement of being diffraction limited at 2 μm without any specific requirement on the optical quality on shorter wavelengths. However, its large aperture (guaranteeing a small core for the Point Spread Function, hereafter PSF), combined with a sampling of 32 mas in NIRCam's short wavelength channel will make JWST an exciting, highly capable followup to the Hubble Space Telescope (HST).

The stellar population science of which JWST is capable will remain fresh, as we have discovered more evidence that halos are built by accretion, and are a complex mix of age and metallicity. Stellar populations science can test the CDM paradigm and reveal further insights into the star formation history of galaxies, and in this case, beyond the boudaries of the Local Group. JWST will offer a breakthrough in advancing the stellar populations studies of Spitzer - especially mass loss in evolved stars - to an unprecedented volume, likely to the Virgo Cluster. This will open up the possibility of exploring star formation histories for thousands of galaxies, to distances of 10 Mpc and beyond.

In this document, we will provide a description of work that we expect to be important in the next decade for which JWST can make important contributions. Broadly speaking one can subdivide this into two distinct categories. For a number of projects the great near-infrared sensitivity of JWST will be a major asset. For others, observations will have to take place at optical wavelengths where the atomic physics of stellar atmospheres places important diagnostics. We will show how even an infrared-optimized JWST, thanks to its larger aperture, will be able to improve over what is possible with HST at the wavelengths where it can operate.

2. Themes

Three major themes that we will focus on are: (1) the study of the star formation histories of nearby galaxies exploting the large lever arm provided by visible-infrared colors (see §3); (2) the derivation of the properties of stellar populations from the study of the bright red stellar component out to the Virgo cluster and beyond (see §4); and (3) the derivation

of the white dwarf (WD) cooling sequence age of globular cluster in the Milky Way from the study of deep visible red color magnitude diagrams (see §5). Table 1 summarizes to what distances the science can be accomplished.

Theme	Distance	Main Wavelength
Star formation histories	Up to 4 Mpc	Visible-near IR
Study of the bright red stars	Up to 40 Mpc	Infrared
WD cooling sequence	Up to 5.3 kpc	Visible

Table 1 : JWST Science themes in the study of stellar populations. The table gives the distance to which the science in each theme can be accomplished and the required wavelength interval.

3. Star Formation Histories

JWST will observe the birth of galaxies at high redshift, but it will complement that research by reconstructing the star formation histories of nearby galaxies, using multi-band photometry of their resolved stellar populations. In a complex population hosting a mix of chemical abundances and ages, an accurate star formation history can be reconstructed from photometry reaching well below the turnoff of the stellar main sequence. For decades, such stars could be resolved only within nearby star clusters of our own Galaxy, but in the 1990s, this technique was pushed into the Milky Way satellites. With a repaired ACS and/or WFC3, the Hubble Space Telescope (HST) can probe star formation histories (SFH) anywhere in the Local Group, including the closest spiral galaxy to our own, M31 (Brown et al. 2006, 2007). However, this work is observationally expensive, and only a few sightlines through Local Group galaxies can be pursued within the remaining HST mission.

JWST will greatly expand upon this work, providing many more measurements of relatively nearby galaxies and by reaching galaxies beyond the Local Group. Although it is not widely appreciated, the broad filters on its near-infrared camera (NIRCam) will provide a more sensitive temperature lever than the most widely-used filters employed for deep HST imaging, thus providing better age diagnostics (Figure 1). Furthermore, JWST will combine HST resolution with a much larger aperture. Surveys of nearby populations will be nearly 6 times faster, while deep surveys can reach galaxies 50% further away (Figure 2). JWST will enable a comprehensive survey of SFH within the Local Group, and probe the members of Sculptor, the galaxy group nearest to our own.

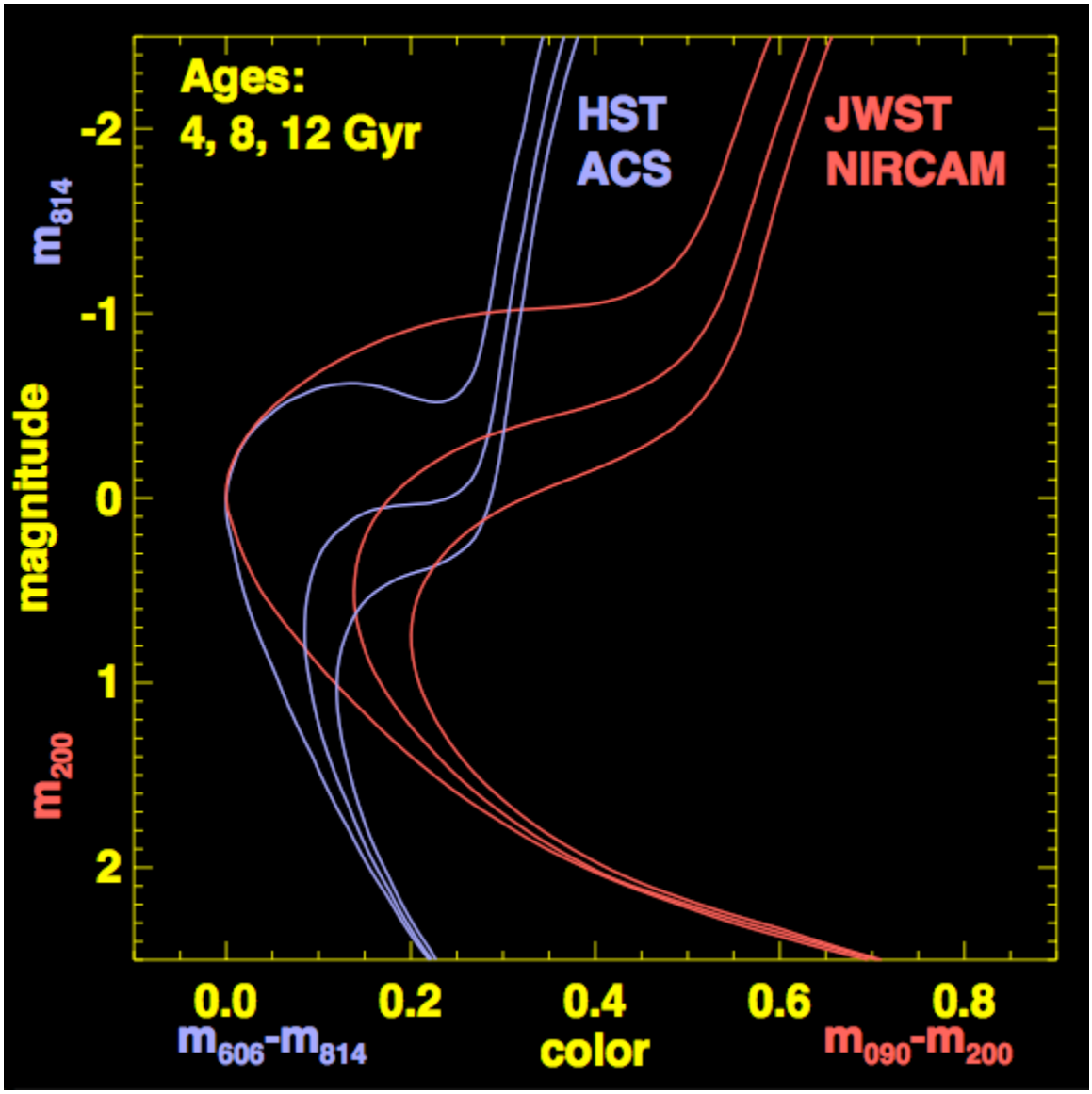

Figure 1: A set of isochrones showing the distribution in color and luminosity for a resolved stellar population at ages of 4, 8, and 12 Gyr. The isochrones are shown in both the ACS filters (F606W & F814W; blue) and JWST/NIRCam filters (F090W and F200W; red) appropriate for deep color-magnitude diagrams. The separation in color with varying age is 65% larger in the JWST filters, yielding more accurate age measurements from such photometry. To ease comparison of the HST and JWST isochrone sets, the zeropoint for each bandpass has been chosen to place the Main Sequence Turn-Off at color=0 and magnitude=0 for a 4 Gyr isochrone.

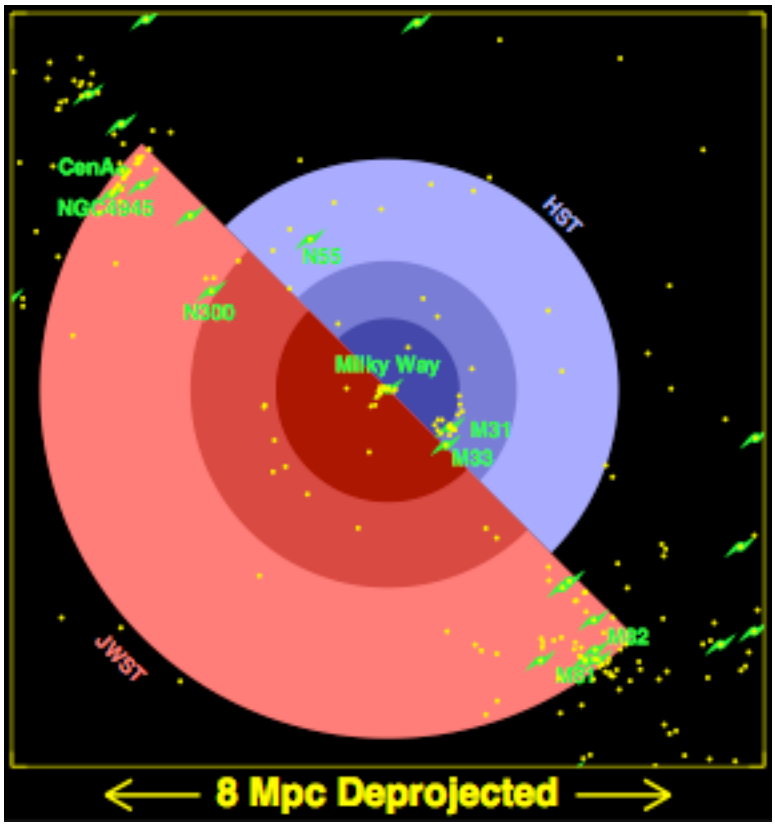

Figure 2: The distribution of galaxies in the nearby universe (yellow points), deprojected to indicate true distances from the Milky Way (center). Spirals brighter than -17 mag and ellipticals brighter than -19 mag are highlighted (green symbols). Concentric circles indicate the volume of space that can be surveyed in 10, 100, and 1000 hours with JWST (red) and HST (blue), reaching 0.5 mag below the turnoff in a 12 Gyr population. HST can survey a few Local Group sightlines, while JWST can survey many Local Group galaxies and also reach the Sculptor Group (e.g., NGC300 and NGC55).

4. Bright Red Stars in Nearby Galaxies

The bright region of the Color-Magnitude Diagram (CMD) of external galaxies carries information on their Star Formation History, albeit with a lesser degree of detail than the turn off region. Indeed the portion of the CMD brighter than $M_J \approx -4$ contains in their evolved evolutionary stages stars formed since one Hubble time. Decoding the stellar counts in this part of the CMD in terms of SFH is complicated by several effects, which include the relatively low number of stars per unit mass of the parent stellar population, the less accurate color temperature transformations, and the uncertain modelling of the Asymptotic Giant Branch (AGB) evolutionary phase. Still, it is possible to derive a robust measurement of the mass in stars within broad age ranges, which corresponds to a

sketch of the SFH up to the Hubble time (Greggio 2002).

Figure 3 illustrates that 10 Gyr old stars can be sampled at $M_J \approx 3$, when on the late Main Sequence (MS) stage, at $M_J \approx -0.5$, when in the core He burning Horizontal Branch phase (HB), or at $M_J \leq -4$ in the bright Red Giant Branch (RGB) and AGB stages. For a given instrumental set up and exposure time, this gain in magnitude enables us to probe old stars in an ~125 times larger volume when using HB stars, or in an ~16000 times larger volume, when relying on the RGB stars, compared to the old MS turn offs.

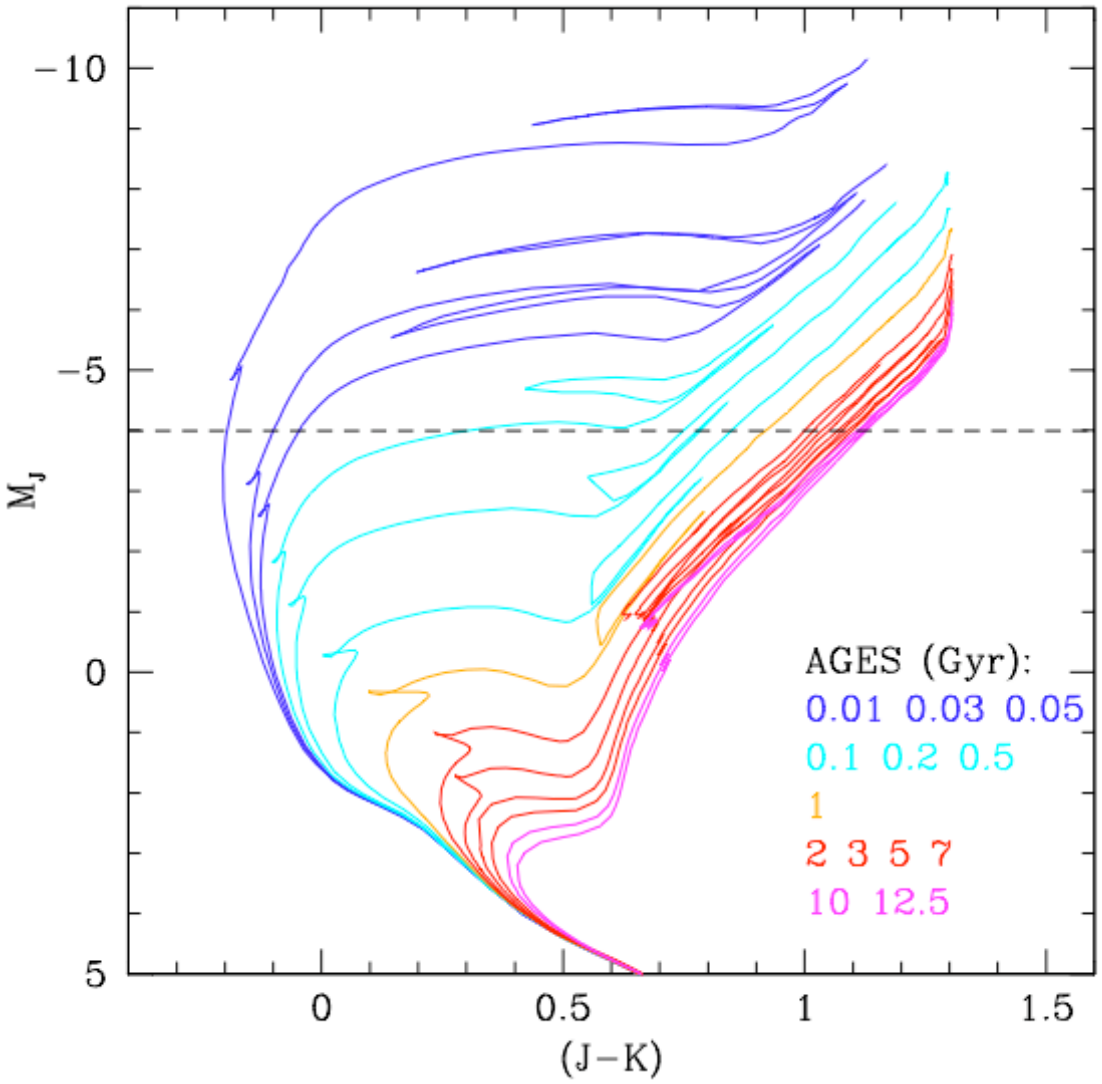

Figure 3. Isochrones with solar metallicity from Girardi et al. 2002 in the Johnson-Cousins-Glass photometric system. The portion of the CMD brighter than -4 samples stars of all possible ages: young stars in the core Helium burning phase; intermediate age stars in the AGB phase and old stars in both the RGB and AGB phases.

Photometry of resolved stars in this bright portion of the CMD allows us to investigate on several important astrophysical problems, namely:

4.1 Accurate distances for distant galaxies from the tip of the RGB

In composite stellar populations, with a range of ages and metallicities, the tip of the RGB stands out as a prominent feature, recognizable as an edge in the stellar counts. For a population with a metallicity spread, the metallicity dependence of the RGB tip absolute magnitude causes the tip of the RGB to trace a linear edge on the CMD, as seen in Cen A (e.g. Rejkuba et al. 2005). Locating this edge on the CMD of galaxies allows us to derive an accurate distance.

4.2 Metallicity distributions of Old Stellar Systems

The color of RGB stars is very sensitive to their metal content; a composite stellar population is charaterized by a broad RGB, and the distribution in color of the stars reflects the metallicity distribution. Age effects can be an issue in this application, since younger stars with large metallicity appear to have similar color as older, less metal rich stars. Still, colors of RGB stars are much more sensitive to metallicity than to age, so that a reasonable determination of the metallicity distribution can be done in spite of the age metallicity degeneracy (e.g. Rejkuba et al. 2005).

Observations of the main-sequence turnoff will provide the most detailed constraints on metallicity, but such observations are expensive, and are likely to be done only for a few sightlines through galaxies beyond the local group. Observations of red-giant branch (RGB) stars are much easier and can potentially be carried out for hundreds of galaxies out to distances beyond the Virgo Cluster. For old stellar populations, the RGB is a good metallicity indicator. Hence systematic studies of the RGB can help us to understand the formation history of galaxies by allowing us to follow the metal content of galaxies from high redshift down to the present.

Valenti et al. (2004, 2007) identify and calibrate infrared features in the RGB that are useful for metallicity determination (Figure 4). The luminosity, color, and slope of the RGB as well as the color and luminosity of the RGB bump all provide metallicity information. Of these, the color of the RGB is the most straightforward to use for composite stellar populations: the shape of the *blue edge* of the RGB provides an important probe of the distribution of very metal poor stars. The other metallicity indicators can be used in studying extragalactic globular clusters in uncrowded fields, but will be difficult to measure in a stellar population that has a wide metallicity distribution.

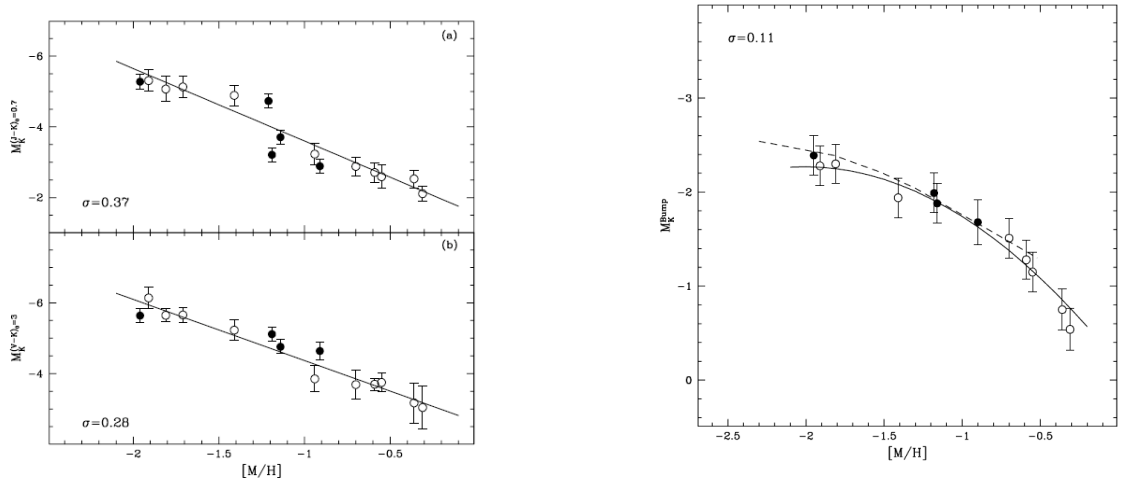

Figure 4. Left: Absolute magnitude of the RGB at fixed color in a sample of Galactic globular clusters. The top panel is for J-K(Vega)= 0.7. The bottom panel is for V-K(Vega) = 3. Right: Absolute magnitude of the RGB bump as a function of metallicity. The solid curve is the best fit. The dashed curve is the theoretical prediction of Straniero et al. (1997). From Valenti et al. (2004). Such comparisons to Galactic globular clusters suggest that the RGB trends at low metallicity are well behaved and well matched by theoretical models.

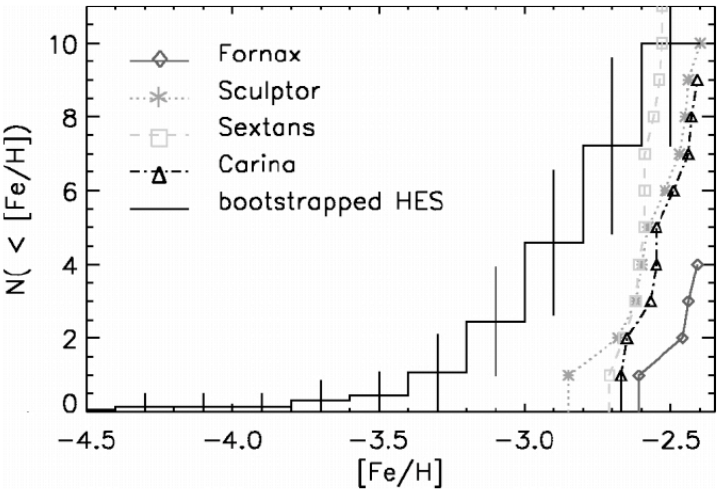

Figure 5. Cumulative metallicity distribution function for stars in dwarf spheroidal galaxies and in the Galactic halo (from the Hamburg/ESO survey). From Helmi et al. 2006.

To use the RGB to constraint the metallicity distribution, it is important to get at least as faint as K(AB) = -2 (see Figure 4, left panel), which requires at 3-hour exposure to reach S/N=10 at the distance of the Virgo Cluster. Similar exposure times can reach K(AB) = 1 at a distance of 4 Mpc, getting beyond the RGB bump and providing more stars and greater color leverage for constraining the metallicity distribution. These observations can only be carried out in low-surface-brightness regions of galaxies, due to crowding.

In a simple closed-box model of chemical evolution ending at solar metallicity, 20% of the population should have [Fe/H] < -1.5. In nearly all actually stellar populations, this fraction is much smaller. Recent studies have revealed that the metallicity distribution shows considerable variety (Figure 5). Detailed comparison of these distributions to models will help constrain the amount of infall and outflow during the early epochs of galaxy formation, and hence provide vital information on the mechanisms that govern and limit star formation.

4.3 SFH in late type galaxies

Figure 6 shows a synthetic CMD of a 3×10^8 solar masses stellar population obtained with a constant SF over a 12 Gyr lifetime. The color encoding reflects the stellar ages. Superimposed are diagnostic boxes, designed to sample well defined age ranges. The number of stars counted within each box is proportional to the mass transformed into stars within the age range sampled by the box. For example, for a Kroupa IMF, in the upper right, upper left, lower right and lower left boxes there should be approximately 10,3,40 and 10 stars per 10^5 solar masses of the parent stellar population in the relative age ranges. Simple stellar counts can thus be translated into stellar mass (modulo an IMF), in different age ranges. This corresponds to deriving a first order description of the SFH in a galaxy. An improved evaluation of the SFH can be obtained via simulations of the CMD, starting from this first approximate solution.

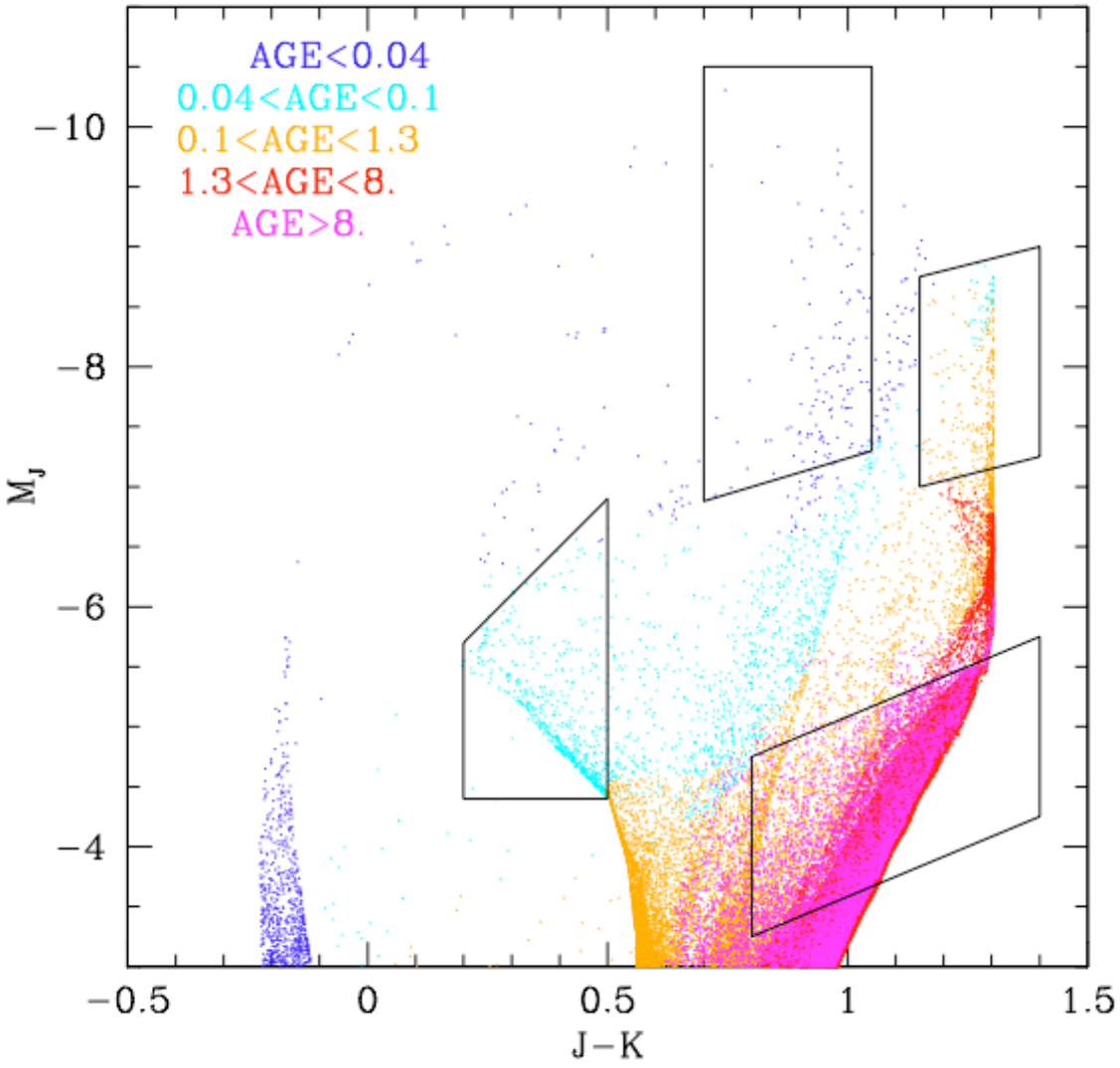

Figure 6. Simulation of a CMD of a stellar population of 3 $\times 10^8$ solar masses obtained with a constant SFR over 12 Gyrs and an age-metallicity relation, with Z increasing linearly to reach the solar value in the first 5 Gyr, while in the subsequent 7 Gyr the growth is much more modest. The colors encode the ages of the synthetic stars. The boxes superimposed have been drawn to sample specific age ranges. The total magnitudes of this population are M_J ≈-17, M_K ≈-18. The simulation has been computed with the code ZVAR by G. Bertelli (priv. Comm.)

4.4 Size and metallicity of the population of intracluster stars

It is well known that the Intra Cluster medium contains a sizable population of old stars (Ferguson, Tanvir & von Hippel 1998), whose census requires large field of view (FOV). The same issues discussed above for the stars in galaxies can be applied to this elusive stellar population, to assess its size, and metallicity distribution. These properties

are important constraints to the evolution of galaxies in clusters including galaxy interactions. In fact, galaxy interactions strip stars from galaxies but the stripped stars generally remain bound to the cluster. The size of the intracluster population can be used to constrain the number and intensity of past galaxy interactions while their properties may be used to constrain the epoch of the last major interaction.

5. The White Dwarf Cooling Sequence in Globular Clusters

Globular star clusters are the oldest systems for which an age may be measured based on well understood stellar evolution timescales. As such, these stellar systems preserve the first well documented era of star formation in the Galaxy and indeed in the Universe. A lower limit to the age of the Universe from these clusters has been and still is an important cosmological constraint. The age of the Universe, 13.7 ± 0.2 Gyr, is derived from measurement of the angular power spectrum of the cosmic microwave background (WMAP; Spergel et al. 2003). However, this age depends on the details of modeling the microwave background power spectrum and also on additional measurements of large scale structure. Thus, there continues to be great value in any independent measurements constraining the age of the Universe, as the authors of the WMAP study emphasize (Spergel et al. (2003)). A measured lower limit to the age of the Universe from stars is an important cosmological parameter with broad implications.

Being the oldest known stellar aggregates, accurately age-dating globular clusters can potentially answer two additional intriguing questions: a) did they form before or after cosmic re-ionization, and in case what part did they play in it? And, b) otherwise, did they form at the time of the formation and assembly of the Galactic spheroid (halo and bulge)? The younger open clusters provide a more recent view of star formation within the Galaxy and simultaneously provide exquisite tests of stellar evolution theory.

The most commonly used method of age-dating the globular clusters is based on the luminosity of the main sequence turnoff, with the uncertainty in the cluster distance modulus dominating the error budget. As a rule of thumb, the relative age uncertainty is nearly equal to the error in distance modulus, e.g. an 0.1 magnitude error in modulus yields a ~10% error in age. In a recent attempt at getting accurate ages with detailed spectroscopy coupled with wide and narrow band photometry, Gratton et al. (2003) estimated distance modulus errors of 0.07 mags and random age errors of 1 Gyr for three nearby clusters. One of these three, 47 Tuc, was found to be 2.6 Gyr younger than the two halo clusters NGC 6397 and NGC 6752 and may be suggesting a substantial age-metallicity relation in the Galaxy providing an important clue to its early formation history.

Reddening and distance uncertainties will continue to be a concern even if trigonometric distances are derived to a handful of nearby clusters by GAIA and the Space

Interferometry Mission. In addition, uncertainties in some of the input physics (such as opacities, gravitational settling, nuclear reaction rates) will continue to be a source of systematic error in these age determinations, which currently are nearly as large as the distance-induced errors (i.e., ~1 Gyr).

A different technique to determine globular cluster ages has recently become possible with deep HST imaging in two of these clusters (Richer et al. 2002, 2006; Hansen et al. 2004, 2007). This is the white dwarf cooling age method, whereby the age is derived from modeling the distribution of white dwarfs in the cluster color-magnitude diagram. Figure 7 illustrates the sensitivity of the appearance of the white dwarf cooling sequence to age. The method is less sensitive to distance and reddening uncertainties, but has its own set of difficult physics (among these are neutrino losses, sedimentation of carbon and oxygen, crystallization and collision induced opacities). Besides uncertainties in white dwarf physics, assumptions on the pre-white dwarf evolution will also affect the results (e.g. the initial-final mass relation, the chemical stratification such as the carbon/oxygen ratio in the WD core, and the mass of the outer helium and hydrogen layers). The important point here is that the physics entering into models of cooling white dwarfs is generally different from that input into main sequence models, so that ages of a given cluster determined with both techniques can provide some estimate of these systematics. For a fixed set of white dwarf cooling models (no systematics investigated for a range of models) Hansen et al. (2007) have derived a cooling age for the globular cluster NGC 6397 with an error of 0.5 Gyr. The use of the white dwarf method is still in its infancy, and only its application to as many clusters as possible can solidify its effectiveness, assess the systematics, and provide a detailed, quantitative understanding of stellar evolution from the main sequence all the way to the faintest remnants.

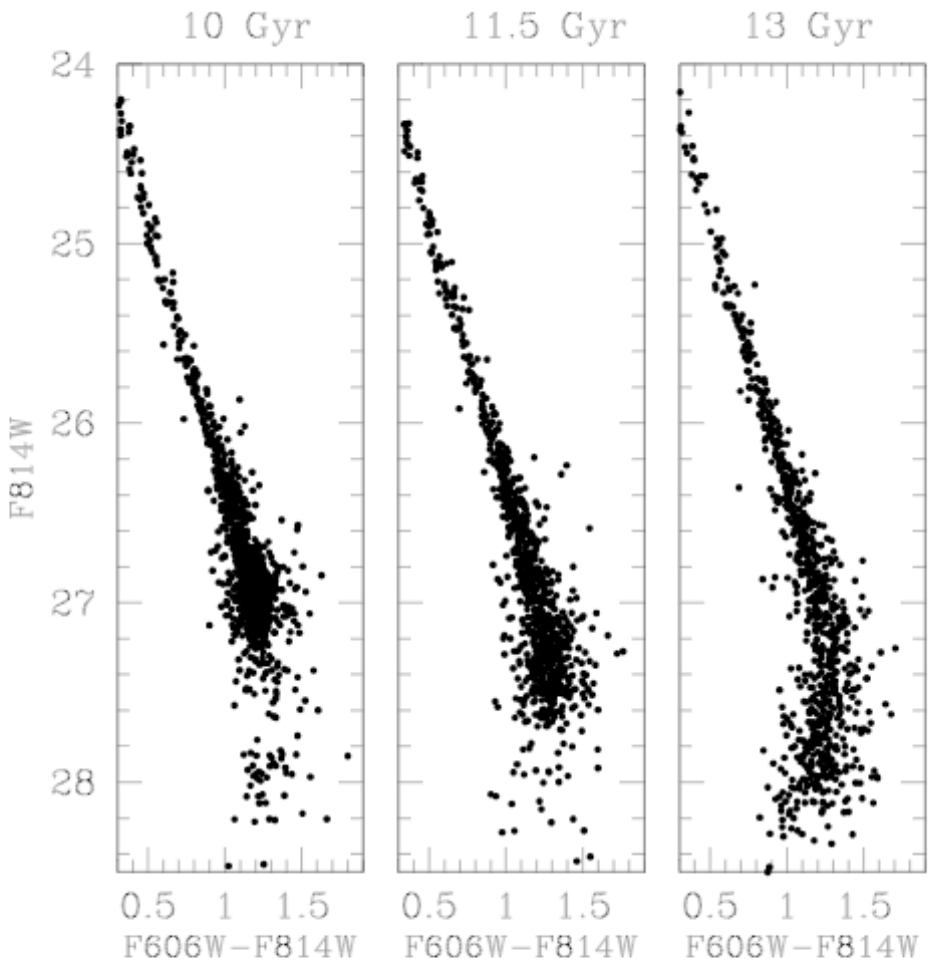

Figure 7 : Realizations of the WD cooling sequence in the HST/ACS filters F606W and F814W (Hansen et al. 2007). The distance and reddening are for NGC 6397 for a cluster age of 10 Gyr (left), 11.5 Gyr (middle), and 13 Gyr (right). This illustrates the strong dependence of the appearance of the cooling sequence on cluster age.

Even with a repaired ACS, Hubble will at best only be able to observe an additional one or possibly two globular clusters down to the truncation in the WD cooling sequences (47 Tuc (if it is young) and NGC 6752 (difficult, requiring 200+ orbits)). A wider sample of clusters awaits JWST. In this case clusters with a range of metallicities and dynamical parameters can be observed to the expected truncation in their WD cooling sequences. With such a large sample and precise cluster ages we will be able to begin to probe cluster formation on the order of the dynamical time scale in the Galactic halo.

Table 2 provides a sample list of potentially observable clusters based on an age of 12 Gyr and the WD DA cooling sequence for hydrogen-rich WDs in the JWST filters shown in Figure 8.

Cluster (1)	Distance (kpc)	AV (mag)	F070W/F090W Truncation	Exp Time (hours) (2)
NGC 104 (47 Tuc)	4.5	0.13	30.1/30.3	24
NGC 5139 (Omega Cen)	5.3	0.38	30.6/30.8	59
NGC 6656 (M22)	3.2	1.09	30.0/30.1	18
NGC 6752	4.0	0.13	29.8/30.1	15
NGC 6809	5.3	0.26	30.5/30.8	55
NGC 6838	4.0	0.80	30.3/30.4	31

Table 2. Sample Globular Cluster WD Cooling Sequence Truncations and Exposure Times. (1) Cluster properties from Harris 1996. (2) Exposure time is the time for JWST to reach the truncation magnitude for WDs with a S/N = 4 in both the F070W and F090W filters. The magnitudes are all Vega magnitudes assuming mag = 0 for Vega in these filters. The extinction ratio F070W/E(B-V) was taken to be the average of the ACS/WFC F606W and F814W ratios while the F090W ratio was assumed to be the same as that of the ACS/WFC F850LP filter.

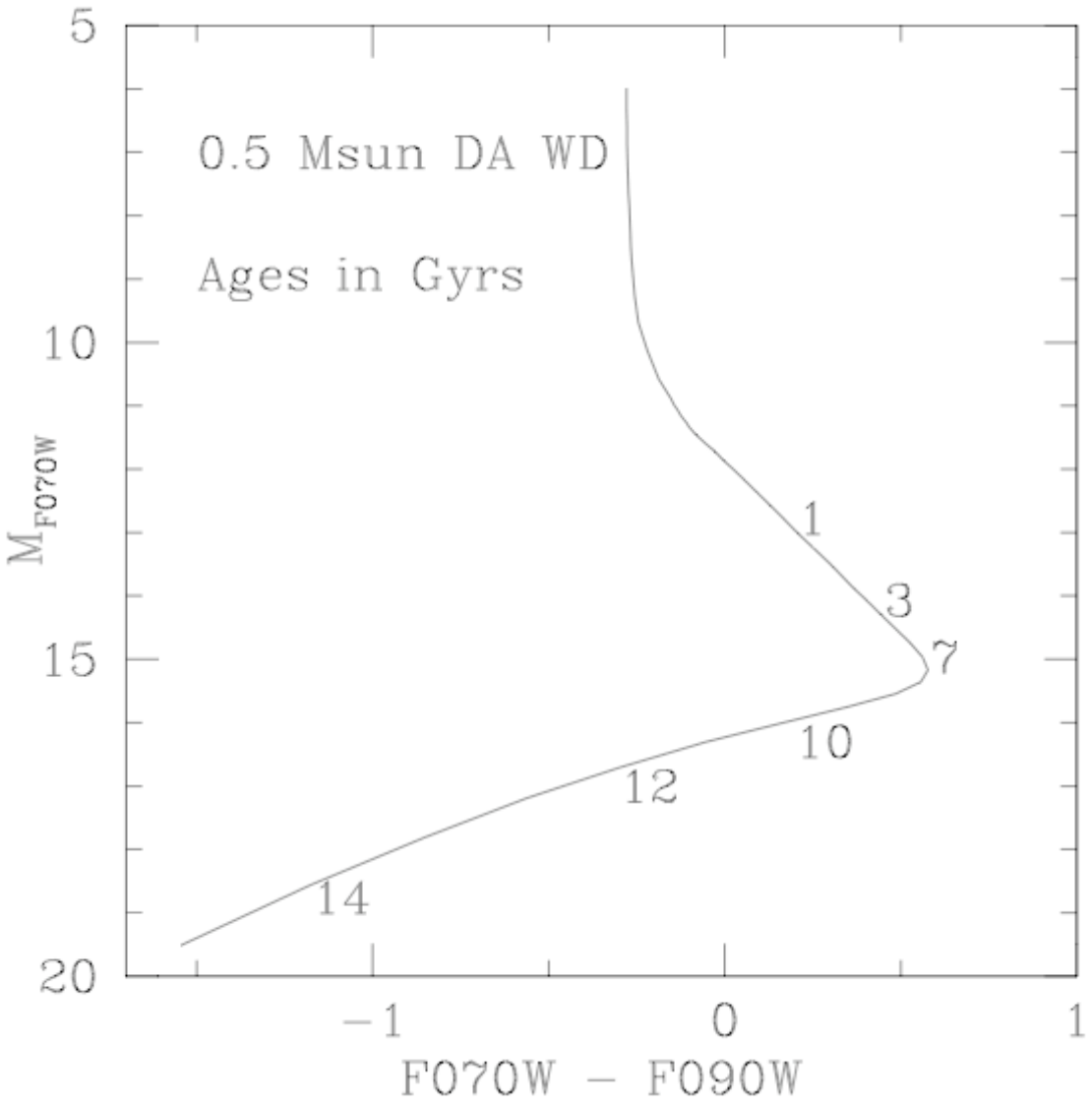

Figure 8. The WD cooling sequence in the JWST filters F070W and F090W. This sequence is for a hydrogen-rich WD with a mass of 0.5 $M_{\odot}$ and was calculated by P. Bergeron.

6. Other science areas

6.1 A Complete Initial Mass Function for Old Stellar Populations

There is growing appreciation that the IMF is likely to be Universal. The Magellanic Clouds (MC) globular clusters span an age range from 10^7 to 10^{10} yr and the properties of brown dwarfs in the younger clusters will be of great interest. Much progress will be made using ground-based AO, but the current limit from the ground is around H=25, while JWST would reach 7 magnitudes fainter. Also, it is unlikely that all of these stellar populations will be properly done (the end of the bulge hydrogen burning sequence will be reached, however, before JWST is launched; this is not the case for the Magellanic Clouds or dwarfs). JWST will be able to measure the IMF for the Galactic Bulge, the Magellanic Clouds and clusters in the MC and the 7 dwarf spheroidals. By doing so it will test the universality of the IMF as a function of metallicity and environment.

6.3 Mid- IR imaging and spectroscopy of resolved AGB populations across the Hubble Sequence.

Figure 8 shows clearly resolved sources in M32 at 8um using Spitzer (Rich et al. 2008, see also Barmby et al. 2006). JWST will have 10x this spatial resolution and much greater sensitivity; images like this will be feasible for any spheroid out to ~20 Mpc (i.e. reaching the Virgo cluster). Differences in the luminosity function and chemistry of AGB populations may correspond to interesting subtleties like minority intermediate age stellar populations or even small age differences. There has been a long standing controversy about the ages of elliptical galaxies; the importance of minority populations vs. possible late formation and evolution to the red sequence (Bell et al. 2004; Faber et al. 2006) are important issues. The age/metallicity degeneracy makes it hard to diagnose minority populations from optical spectra, so the mid-IR populations are most promising as a means of discriminating fine age differences in old stellar populations.

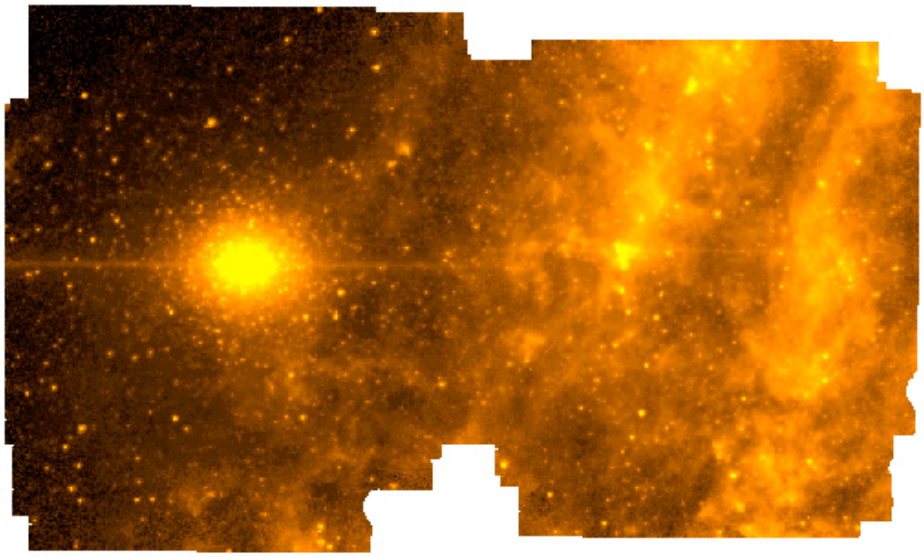

Figure 8. Spiter IRAC observations of M32 at 8mm. Clearly visible are a multitude of resolved sources (Rich et al. 2008)

7. Summary

The James Webb Space Telescope will make important contributions to the study of resolved stellar populations. JWST will be able to study the star formation histories of nearby galaxies exploiting the large lever arm probided by visible-infrared colors. It will enable to use bright red evolved stars to study stellar populations out to the Virgo Clusters and it will enable the derivation of the white dwarf cooling sequence age of several globular clusters not presently accessible with HST. These projects require high sensitivity and good angular resolution with a stable point spread function and are ideally suited to JWST capabilities. Here we have focused on imaging science not because there is no interesting spectroscopic science that could be carried out in this field but because imaging is an area of greater strength of JWST.

References

Barmby, P., et al. 2006, ApJ, 650, L45.
Bell, E. F. 2004, ApJ, 608, 752.
Brown, T. et al. 2006, ApJ, 652, 323.
Brown, T. et al. 2007, ApJ, 658, L95.
Faber, S. M., et al., 2007, ApJ, 665, 265.
Ferguson, H.C., Tanvir, N.R., & von Hippel, T. 1998, Nature 391, 461.
Hansen, B., 2004, ApJS, 155, 551.
Hansen, B, 2007, arXiv:astro-ph/0701738.
Helmi, A, et al. 2006, ApJ, 651, L121.
Girardi, L. et al. 2002, AA 391,195.
Greggio, L. 2002, ASP Conf. Ser. 274, 444.
Rejkuba, M. et al. 2005, ApJ 631, 262.
Rich, M. et al. 2008, in preparation
Richer, H. B., et al. 2002, ApJ, 574, L151.
Richer, H. B., et al. 2006, Science, 313, 936.
Spergel D., et al. 2003, ApJS, 148, 175.
Straniero, O. et al. 1997, ApJ, 490, 425.
Valenti, E., et al., 2004, AA, 419, 139.
Valenti, E. et al., 2007, AJ, 133, 1287.